Articles

Structural Determinants of Nucleotide Coenzyme Specificity in the Distinctive Dinucleotide Binding Fold of HMG-CoA Reductase from *Pseudomonas mevalonii*†

Jon A. Friesen,‡ C. Martin Lawrence,§,|| Cynthia V. Stauffacher,§ and Victor W. Rodwell*,‡

Departments of Biochemistry and Biological Sciences, Purdue University, West Lafayette, Indiana 47907

Received April 25, 1996; Revised Manuscript Received June 24, 1996⊗

ABSTRACT: The 102-residue small domain of the 428-residue NAD(H)-dependent HMG-CoA reductase of *Pseudomonas mevalonii* (EC 1.1.1.88) binds NAD(H) at a distinctive, non-Rossmann dinucleotide binding fold. The three-dimensional structure reveals that Asp146 lies close to the 2′-OH of NAD^+. To investigate the role of this residue in determination of coenzyme specificity, Asp146 was mutated to Ala, Gly, Ser, and Asn. The mutant enzymes were analyzed for their ability to catalyze the oxidative acylation of mevalonate to HMG-CoA using either the natural coenzyme NAD^+ or the alternate coenzyme $NADP^+$. Mutation of Asp146 to Ala or Gly increased the specificity for $NADP^+$, expressed as the ratio of k_{cat}/K_m for $NADP^+$ to k_{cat}/K_m for NAD^+, 1200-fold (enzyme D146G) and 6700-fold (enzyme D146A). Mutation of Asp146 was accompanied by 565-fold (D146G) and 330-fold (D146A) increases in k_{cat}/K_m for $NADP^+$ and 2-fold (D146G) and 20-fold (D146A) decreases in k_{cat}/K_m for NAD^+. To further improve $NADP^+$ specificity, Gln147, Leu148, Leu149, or Thr192 of enzyme D146G or D146A was replaced by lysine or arginine, which could stabilize the 2′-phosphate of $NADP^+$. Enzymes D146G/T192K, D146G/T192R, D146G/L148K, D146A/L148K, and D146A/L148R exhibited 3200-, 4500-, 56 000-, 72 000-, and 83 000-fold increases in the specificity for $NADP^+$ relative to the wild-type enzyme.

Almost all nicotinamide nucleotide-dependent oxidoreductases possess structural elements that clearly discriminate between NAD^+ and $NADP^+$, coenzymes that differ structurally only with respect to the absence or presence of a 2′-phosphate on the adenine ribose. NAD^+ typically serves as the coenzyme for oxidation in catabolic reactions while NADPH serves as the coenzyme for reductive biosynthetic reactions. Different HMG-CoA[1] reductases illustrate this dichotomy. The biosynthetic HMG-CoA reductases (EC 1.1.1.34) of eukarya (Rodwell *et al.*, 1976; Brown & Rodwell, 1980) or of archaea (Cabrera *et al.*, 1986; Bischoff & Rodwell, 1996) utilize NADPH to reduce HMG-CoA to mevalonate (reaction 1) for ultimate synthesis of isoprenoids such as cholesterol.

(*S*)-HMG-CoA + 2NADPH + $2H^+$ → (*R*)-mevalonate + CoASH + $2NADP^+$ (1)

By contrast, the biodegradative HMG-CoA reductase of *Pseudomonas mevalonii* (EC 1.1.1.88) utilizes NAD^+ in the oxidative acylation of mevalonate to HMG-CoA (reaction 2), the first reaction of mevalonate catabolism in *P. mevalonii* (Gill *et al.*, 1985; Beach & Rodwell, 1989).

(*R*)-mevalonate + CoASH + $2NAD^+$ → (*S*)-HMG-CoA + 2NADH + $2H^+$ (2)

The three-dimensional structure of *P. mevalonii* HMG-CoA reductase (Lawrence *et al.*, 1995) reveals a dimer with two active sites, each of which includes residues contributed by both subunits. Each monomer has two domains, the larger of which binds HMG-CoA and contributes residues that function in catalysis and the smaller of which binds NAD(H). In contrast to lactate dehydrogenase (LDH, EC 1.1.1.27), glyceraldehyde-3-phosphate dehydrogenase (GPDH, EC 1.2.1.12), or alcohol dehydrogenase (ADH, EC 1.1.1.1), enzymes whose NAD^+-binding domains are located at either their N-terminus (LDH, GPDH) or C-terminus (ADH), the more central NAD^+-binding domain of *P. mevalonii* HMG-CoA reductase is formed by residues 110−212 of the 428-residue monomer.

Many NAD^+-dependent oxidoreductases possess an approximately 140-residue Rossmann dinucleotide binding fold, a structure consisting of a parallel, six-stranded β-sheet composed of a pair of $\beta-\alpha-\beta-\alpha-\beta$ elements linked by right-handed crossover connections (Figure 1, right). The

†Funded by National Institutes of Health Grants HL 47113 (V.W.R.) and HL 52115 (C.V.S.) and by a predoctoral fellowship awarded to J.A.F. by the American Heart Association, Indiana Affiliate. The data are derived in part from the Ph.D. thesis of J.A.F. This is journal paper 15038 from the Purdue University Experiment Station.

* To whom correspondence and requests for reprints should be addressed. Tel: 317-494-1608/6. Fax: 317-494-7897. Email: rodwell@biochem.purdue.edu.

‡Department of Biochemistry, Purdue University.

§ Department of Biological Sciences, Purdue University.

|| Present address: Howard Hughes Medical Institute and Laboratory of Molecular Medicine, Children's Hospital, Boston, MA 02115.

⊗ Abstract published in *Advance ACS Abstracts,* September 1, 1996.

[1] Abbreviations: NAD, nicotinamide adenine dinucleotide; CoA and CoASH, coenzyme A; DEAE, diethylaminoethyl; HMG, 3-hydroxy-3-methylglutaryl; PCR, polymerase chain reaction. For k_{cat} and K_m values, the suffixes NAD and NADP refer to the form of the coenzyme used.

S0006-2960(96)00993-2 CCC: $12.00

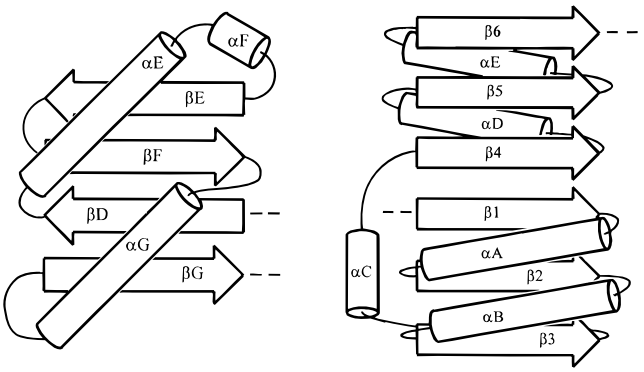

FIGURE 1: Comparison of secondary structural elements of nucleotide-binding domains. Left: nucleotide-binding domain of *P. mevalonii* HMG-CoA reductase. Right: a classical Rossmann dinucleotide-binding domain.

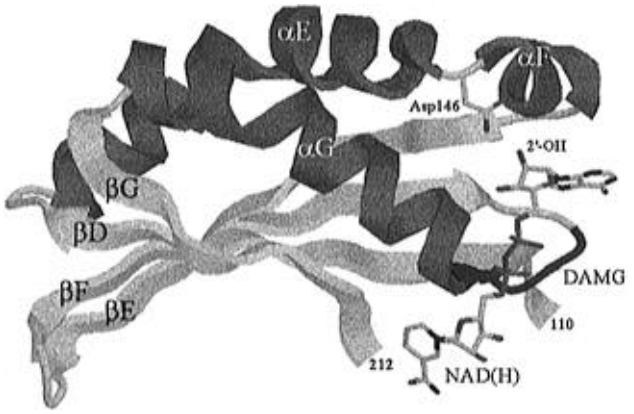

FIGURE 2: Three-dimensional structure of the nucleotide-binding domain of *P. mevalonii* HMG-CoA reductase. The ribbon diagram was constructed using RasMol v2.6β (Sayle, 1995). Shown is the DAMG sequence (green), conserved in all HMG-CoA reductases, formed by residues 183−186, Asp146, and the structure of NAD(H).

approximately 30-residue β1−αA−β2 structure contains a GxGxxG motif which starts helix αA, whose N-terminal dipole stabilizes the pyrophosphate of NAD(H). A conserved aspartate forms a hydrogen bond with the 2′-hydroxyl of the adenine ribose of NAD(H) and facilitates discrimination between NAD(H) and NADP(H) (Rossmann *et al.*, 1975).

The NAD(H)-binding fold of *P. mevalonii* HMG-CoA reductase consists of an interdigitated four-stranded, antiparallel β-sheet with right-handed crossover helices that lie on only one side of the sheet (Figure 1, left). This dinucleotide binding fold differs from a classical Rossmann fold and from the non-Rossmann dinucleotide binding folds of the decarboxylating dehydrogenases (Chen *et al.*, 1995), 6-phosphogluconate dehydrogenase (Rowland *et al.*, 1994), or medium-chain acyl-CoA dehydrogenase (Kim & Wu, 1988). Although the *P. mevalonii* nucleotide-binding domain has no GxGxxG motif, Gly186 of the conserved DAMG sequence appears to correspond to the second glycine of the GxGxxG motif of a Rossmann fold, for Gly186 is located at the N-terminus of helix αG whose N-terminal dipole moment stabilizes the negatively charged pyrophosphate of NAD(H) (Figure 2). In addition, Asp146 of the αE−αF loop may perform a function analogous to that of the invariant aspartate of a Rossmann NAD-binding fold, forming a hydrogen bond to the 2′-hydroxyl of the adenine ribose and discriminating between NAD(H) and NADP(H). This correspondence suggested that removal of bulk, charge, or hydrogen-bonding capability at position 146 might eliminate steric hindrance or charge repulsion of the 2′-phosphate of NADP(H) and enhance the ability of the *P. mevalonii* enzyme to use NADP(H) as coenzyme.

Guided by the three-dimensional structure and by sequence alignments with biosynthetic HMG-CoA reductases that utilize NADPH, we have investigated potential specificity determinants of the unique dinucleotide binding fold of *P. mevalonii* HMG-CoA reductase.

EXPERIMENTAL PROCEDURES

Chemicals. Purchased reagents include DEAE-Sepharose (Sigma), T4 DNA ligase (Promega), a Sequenase kit (USB), restriction enzymes (New England Biolabs, Promega, or Gibco), vent DNA polymerase (New England Biolabs), [α-^{35}S]dATP (Amersham), and a Qiaex gel extraction kit (Qiagen).

Site-Directed Mutagenesis. Mutant genes were constructed using the PCR-based overlap extension method of oligonucleotide-directed mutagenesis (Mikaelian & Sergeant, 1992). Oligonucleotides were synthesized in the Purdue University Laboratory for Macromolecular Structure and purified either by thin-layer chromatography or by polyacrylamide gel electrophoresis. All mutations were verified by DNA sequencing.

DNA Sequencing. The Sanger dideoxy chain termination method (Sanger *et al.*, 1977) used for sequencing employed a USB Sequenase kit and [α-^{35}S]dATP. Mutant genes were subcloned into M13mp19 for generation of single-stranded template DNA.

Overexpression and Purification of Enzymes. Escherichia coli BL21 cells harboring expression vector pHMGR (wild-type or mutant) (Beach & Rodwell, 1989) were grown at 37 °C, with shaking at 300 rpm, in LB medium (Sambrook *et al.*, 1989) that contained 50 μg/mL ampicillin. Wild-type and mutant enzymes were purified through the DEAE fraction as previously described (Wang *et al.*, 1990).

Spectrophotometric Assay of HMG-CoA Reductase Activity. The formation of NAD(P)H that accompanied the oxidation of mevalonate by HMG-CoA reductase was monitored at 340 nm in a Hewlett-Packard Model 8452A diode array spectrophotometer equipped with a cell holder maintained at 37 °C. Assays contained, in 150 μL, 4 mM (*R*,*S*)-mevalonate, 1 mM coenzyme A, from 0.02 to 10 mM NAD^+ or $NADP^+$, 0.1 M KCl, and 0.1 M Tris-HCl, pH 9.0. Reaction mixtures containing all components except mevalonate were first monitored to detect any mevalonate-independent reduction of NAD^+ or $NADP^+$. Reactions were then initiated by adding mevalonate. One unit of HMG-CoA reductase activity is defined as the amount of enzyme that catalyzes the reduction of 1 μmol of $NAD(P)^+$/min.

Determination of Kinetic Parameters. pH profiles were determined in 100 mM Tris, 100 mM K_xPO_4, and 100 mM glycine adjusted to the desired pH, measured at 37 °C, with KOH or HCl. K_m and V_{max} at pH 9.0 (wild-type and mutant enzymes) or at pH 6.0 (wild-type enzyme) were determined for NAD^+ or $NADP^+$ from double-reciprocal plots of $1/v_i$ versus 1/[S]. k_{cat} is defined as V_{max} divided by the molar concentration of active sites, two per dimer. k_{cat}/K_m, a measure of catalytic efficiency, was then calculated. To determine whether mutations had altered K_m values for mevalonate or coenzyme A, each mutant enzyme was

	143	152	180	195
P. mevalonii	NRK **D** QLL NSL		DVR **DAMG** ANTVN **T** MAE	
Human	EGF **A** VIK EAF		RSG **DAMG** MNMIS K GTE	
Hamster	EGF **A** VIK DAF		KTG **DAMG** MNMIS K GTE	
Rat	EGF **A** VVN EAF		KTG **DAMG** MNMIS K GTE	
Sea Urchin	ENF **A** AIK ERF		LTG **DAMG** MNMIS K GTE	
H. volcanii	DNF **A** ALK EAA		DTK **DAMG** MNMAT I ATE	

FIGURE 3: Alignment of sequences of representative HMG-CoA reductases. The underlined residues, Asp146, Q147, L148, L149, and T192 of *P. mevalonii* HMG-CoA reductase, were probed by site-directed mutagenesis. Alignments were produced by the Pileup program of the Wisconsin package (Devereux *et al.*, 1984). Gly186 of the conserved DAMG motif (bold) of *P. mevalonii* HMG-CoA reductase begins helix αG, whose N-terminal dipole stabilizes the pyrophosphate moiety of NAD^+.

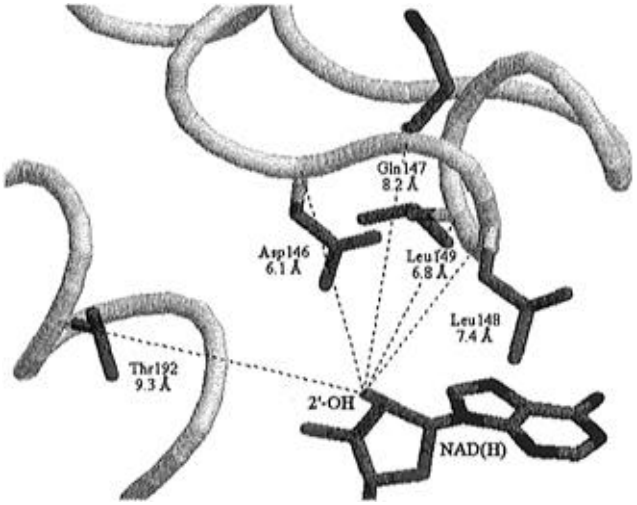

FIGURE 4: Spatial relationship between the 2′-OH of the adenine ribose of NAD(H) and Asp146, Gln147, Leu148, Leu149, and Thr192. The figure was built using RasMol v2.6β (Sayle, 1995). Distances in angstroms are measured from the 2′-OH of NAD(H) to the α-carbon atoms of the mutated residues, calculated in the unrefined structure of the NAD^+:HMG-CoA reductase complex.

assayed at concentrations 5-fold above and 5-fold below the concentration used in the standard assay. In no case did the data suggest altered K_m values for these substrates.

RESULTS

Alignment of the sequences of several biosynthetic NADPH-utilizing HMG-CoA reductases revealed that an alanine occupies the position that corresponds to Asp146 of the *P. mevalonii* enzyme (Figure 3). Alanine, unlike aspartate, could both provide additional space at this position in the structure and eliminate charge repulsion with the 2′-phosphate of NADP(H). Since the α-carbons of Gln147, Leu148, Leu149, and Thr192 are within 6−10 Å of the 2′-hydroxyl of the adenine ribose of NAD(H) (Figure 4), introduction of a positively charged residue at one of these positions thus might stabilize the 2′-phosphate of NADP(H) and hence enhance specificity for $NADP^+$. We therefore also constructed and kinetically characterized derivatives of mutant enzymes D146A or D146G in which Lys or Arg replaced residues Q147, L148, L149, or T192.

Kinetic Parameters for Catalysis by the Wild-Type Enzyme of the Oxidative Acylation of Mevalonate to HMG-CoA Using NAD^+ or $NADP^+$ as Oxidant. For catalysis of reaction 2 by wild-type HMG-CoA reductase using NAD^+ as oxidant, k_{cat} was 27 s^{-1} and K_m for NAD^+ was 0.21 mM. Catalytic efficiency with NAD^+, expressed as $k_{cat(NAD)}/K_{m(NAD)}$, was 130 000 M^{-1} s^{-1}. In terms of both k_{cat} and K_m, $NADP^+$ is an extremely poor oxidant for the wild-type enzyme. $k_{cat(NADP)}$ was 0.04% of $k_{cat(NAD)}$, $K_{m(NADP)}$ exceeded $K_{m(NAD)}$ by a factor of 250, and the ratio $k_{cat(NAD)}/K_{m(NAD)}$ exceeded $k_{cat(NADP)}/K_{m(NADP)}$ by a factor of 5.6×10^5.

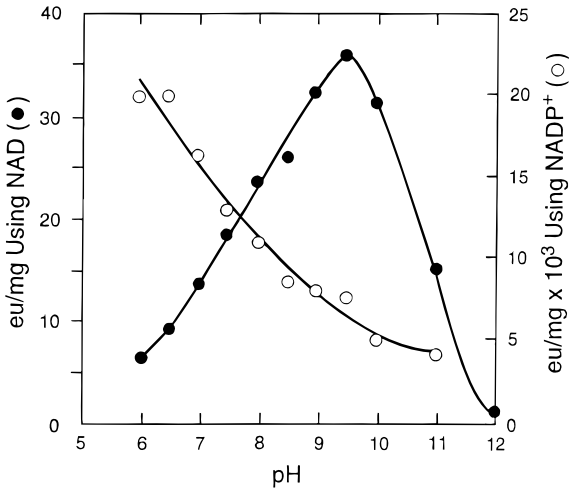

FIGURE 5: pH profiles for catalysis by wild-type *P. mevalonii* HMG-CoA reductase using NAD^+ (●) or $NADP^+$ (○) as oxidant.

Effect of pH on Catalysis. Catalysis of reaction 2 by the wild-type enzyme was optimal at pH 9 using NAD^+, but at a pH below 6 using $NADP^+$ (Figure 5). In addition, $k_{cat(NADP)}/K_{m(NADP)}$ was 23-fold higher at pH 6.0 than at pH 9.0 (Table 1). While for catalysis by the wild-type enzyme $NADP^+$ is a better oxidant at acidic pH, replacement of the negatively charged residue Asp146 by Ala or Gly restored the pH profile using $NADP^+$ to that of the wild-type enzyme using NAD^+ (Figure 6).

Catalysis by Aspartate 146 Single Mutants Using NAD^+ as Oxidant. Asp146 was changed to Ala or Gly to remove charge and reduce bulk, to Asn to remove charge, and to Ser to reduce bulk but retain hydrogen-bonding capability. Substitution of Gly for Asp at position 146 had minimal effect on either $k_{cat(NAD)}$ or $K_{m(NAD)}$. $k_{cat(NAD)}$ remained at the wild-type value while $K_{m(NAD)}$ increased only 2-fold. Substitution of Ala at position 146, while without major effect on $k_{cat(NAD)}$, elevated $K_{m(NAD)}$ 14-fold. Substitution of Asn or Ser for Asp146 decreased $k_{cat(NAD)}$ 37- and 210-fold and increased $K_{m(NAD)}$ 21- and 7-fold, respectively (Table 1).

Catalytic Efficiency of Aspartate 146 Single Mutants Using $NADP^+$ as Oxidant. While mutant enzymes D146N and D146S lacked detectable activity using $NADP^+$, substitution for Asp146 of the smaller, neutral amino acids Gly or Ala profoundly increased the catalytic efficiency with $NADP^+$ and decreased the catalytic efficiency with NAD^+. Mutation of Asp146 to Gly or Ala increased $k_{cat(NADP)}/K_{m(NADP)}$ 565-fold (D146G) and 330-fold (D146A) and decreased $k_{cat(NAD)}/K_{m(NAD)}$ 2- and 20-fold. Increased efficiency with $NADP^+$ was a consequence of both 38-fold (D146G) and 50-fold (D146A) increases in $k_{cat(NADP)}$ and 14-fold (D146G) and 7-fold (D146A) decreases in $K_{m(NADP)}$.

Coenzyme Specificity of Aspartate 146 Single Mutants. Like catalytic efficiency, $NADP^+$ specificity was also profoundly affected by mutation of Asp146 to Ala or Gly.

Table 1: Kinetic Parameters of Wild-Type and Mutant *P. mevalonii* HMG-CoA Reductases[a]

enzyme	$k_{cat(NAD)}$ (s^{-1})	$k_{cat(NADP)}$ (s^{-1})	$K_{m(NAD)}$ (mM)	$K_{m(NADP)}$ (mM)	$k_{cat(NAD)}/K_{m(NAD)}$ (M^{-1} s^{-1})	$k_{cat(NADP)}/K_{m(NADP)}$ (M^{-1} s^{-1})	$\frac{k_{cat}/K_{m(NADP)}}{k_{cat}/K_{m(NAD)}}$	improvement in specificity[b]
wild type	27	0.012	0.21	52	130 000	0.23	1.8×10^{-6}	
wild type, pH 6	ND	0.030	ND	5.7		5.3		
D146G	27	0.46	0.43	3.6	63 000	130	2.1×10^{-3}	1 170
D146A	18	0.60	2.9	7.9	6 200	76	12×10^{-3}	6 670
D146N	0.72	$<10^{-4}$	4.4		160			
D146S	0.13	$<10^{-4}$	1.5		84			
D146A/Q147K	0.60	$<10^{-4}$	2.6		230			
D146A/L148K	3.8	0.16	19	6.1	200	27	130×10^{-3}	72 200
D146A/L148R	0.33	0.14	4.5	13	74	11	150×10^{-3}	83 300
D146A/T192K	0.077	$<10^{-4}$	2.2		36			
D146A/T192R	0.029	$<10^{-4}$	2.8		10			
D146G/L148K	0.42	0.11	18	47	23	2.3	100×10^{-3}	55 600
D146G/L148R	0.16	$<10^{-4}$	28		2.7			
D146G/T192K	0.87	0.020	2.8	11	320	1.8	5.7×10^{-3}	3 170
D146G/T192R	11	0.23	5.2	14	2 000	16	8.1×10^{-3}	4 500

[a] Except where noted for the wild-type enzyme, all data were taken at pH 9. For both NAD^+ and $NADP^+$, k_{cat} for enzymes D146A/L149K, D146A/L149R, and D146A/Q147R was below our limits of detection, $<10^{-4}$ s^{-1}. ND; not determined. [b] Improvement in specificity is the ratio $[k_{cat(NADP)}/K_{m(NADP)}]/[k_{cat(NAD)}/K_{m(NAD)}]$ for a given mutant enzyme divided by $[k_{cat(NADP)}/K_{m(NADP)}]/k_{cat(NAD)}/K_{m(NAD)}]$ for the wild-type enzyme.

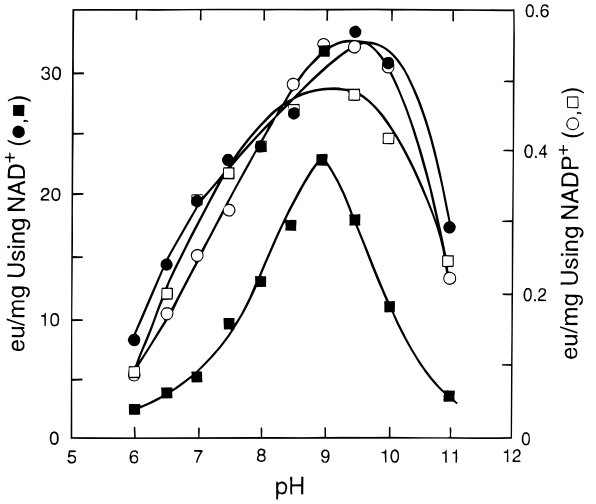

FIGURE 6: pH profiles for catalysis by mutant enzymes D146A (squares) and D146G (circles) with NAD^+ (closed symbols) or $NADP^+$ (open symbols) as oxidant.

The ratio $k_{cat(NADP)}/K_{m(NADP)}$ to $k_{cat(NAD)}/K_{m(NAD)}$, a quantitative measure of $NADP^+$ specificity, was 2.1×10^{-3} for enzyme D146A and 12×10^{-3} for enzyme D146G, increases of 1200- and 6700-fold relative to the ratio for wild-type enzyme of 1.8×10^{-6} (Table 1).

Catalytic Efficiency and Coenzyme Specificity of Double Mutant Enzymes. Inspection of the three-dimensional structure of *P. mevalonii* HMG-CoA reductase suggested that the introduction of a positive charge at position 147, 148, 149, or 192 might stabilize the negative charge of the 2′-phosphate of NADP(H) and further enhance the ability of this enzyme to use $NADP^+$ as coenzyme (Figure 4). We therefore constructed and kinetically characterized derivatives of mutant enzymes D146A or D146G in which Lys or Arg replaced residues Gln147, Leu148, Leu149, or Thr192.

Significant improvement was observed for enzymes D146G/T192K and D146G/T192R, where $NADP^+$ specificity increased 3- and 4-fold relative to enzyme D146G, a result of larger (200- and 32-fold) decreases in $k_{cat(NAD)}/K_{m(NAD)}$ than in $k_{cat(NADP)}/K_{m(NADP)}$ (72- and 8-fold).

For second-site mutations, the greatest improvement in $NADP^+$ specificity resulted from mutation of position 148. For enzymes D146A/L148K and D146A/L148R, $NADP^+$ specificity increased 11- and 13-fold, respectively, relative to enzyme D146A. Decreases in $k_{cat(NAD)}/K_{m(NAD)}$ of 31- and 84-fold were accompanied by decreases in $k_{cat(NADP)}/K_{m(NADP)}$ of only 3- and 7-fold for enzymes D146A/L148K and D146A/L148R, respectively.

The most effective second-site mutation involved substitution of lysine, but not of arginine, for Leu148 of enzyme D146G. The $NADP^+$ specificity of enzyme D146G/L148K increased 48-fold relative to enzyme D146G, a consequence of a 2700-fold decrease in $k_{cat(NAD)}/K_{m(NAD)}$ accompanied by only a 57-fold decrease in $k_{cat(NADP)}/K_{m(NADP)}$. However, substitution of arginine decreased $k_{cat(NAD)}$ 170-fold and rendered enzyme D146G/L148R inactive with $NADP^+$. Substitution of lysine or arginine at position 147, 149, or 192 of enzyme D146A also was ineffective, yielding enzymes with 30−620-fold decreases in $k_{cat(NAD)}$ that either were inactive with $NADP^+$ or had no detectable activity using either coenzyme (Table 1).

DISCUSSION

P. mevalonii HMG-CoA reductase is highly specific for NAD^+, having a catalytic efficiency 6×10^5-fold greater with NAD^+ than with $NADP^+$. The crystal structure of the binary NAD^+:HMG-CoA reductase complex revealed that Asp146 in the αE−αF loop of the nucleotide-binding domain is adjacent to the 2′-hydroxyl of the adenine ribose of NAD^+ and thus may play a critical role in the determination of coenzyme specificity. This appears to be the case, as substitution of alanine or glycine for aspartate at position 146 both diminished catalytic efficiency with NAD^+ and enhanced catalytic efficiency with $NADP^+$. We attribute the decrease in efficiency with NAD^+ to loss of a hydrogen bond between Asp146 and the 2′-hydroxyl of NAD^+. Enhanced ability to use $NADP^+$ would then result both from the elimination of charge repulsion and from the increase in space to accommodate the 2′-phosphate of the unnatural coenzyme. Replacement of Asp146 by Gly or Ala did not appear to severely affect the overall conformation of the NAD^+-binding site since $k_{cat(NAD)}$ for enzymes D146G and D146A were 100% and 67% of the wild-type value. A role for Asp146 in NAD^+ binding was nevertheless suggested by the 2-, 7-, 14-, and 21-fold increases in the K_m for NAD^+

Table 2: Comparison with Other Coenzyme Specificity Studies[a]

enzyme	mutation(s)	improvement in specificity	% wild-type efficiency
NAD(H) to NADP(H)			
P. mevalonii HMG-CoA reductase	D146G	1 170	0.10
P. mevalonii HMG-CoA reductase	D146A/L148R	83 300	0.01
E. coli dihydrolipoamide dehydrogenase[b]	E203V/M204R/F205K/D206H/P210R	NA[l]	126
Drosophila melanogaster ADH[c]	D38N	510	75
Bacillus stearothermophilus LDH[d]	D53S	17	0.19
Saccharomyces cerevisiae ADH I[e]	D223G	NA[l]	0.12
Thermus flavus malate dehydrogenase[f]	E41G/I42S/P43E/Q44R/A45S/M46F/K47Q	520	34
rat dihydropteridine reductase[g]	D37I	2.4	0.5
B. stearothermophilus GPDH[h]	D32A/L187A/P188S	NA[l]	2.0
NADP(H) to NAD(H)			
E. coli glutathione reductase[i]	A179G/A183G/V197E/R198M/K199F/H200D/R204P	17 700	3.3
Thermus thermophilus isocitrate dehydrogenase[j]	R231A/Y284F	120	0.071
E. coli isocitrate dehydrogenase[k]	K334D/Y345I/V351A/Y391K/R395S/C332Y/C201I	1 390 000	3.5

[a] Improvement in specificity is the ratio of the wild-type to mutant values of $[k_{cat(N)}/K_{m(N)}]/[k_{cat(U)}/K_{m(U)}]$ where N is the natural or preferred form of the coenzyme and U is the unnatural or less preferred form of the coenzyme. Percent wild-type efficiency is the ratio of $k_{cat(U)}/K_{m(U)}$ for the mutant enzyme to $k_{cat(N)}/K_{m(N)}$ for the wild-type enzyme multiplied by 100. [b] Bocanegra *et al.*, 1993. [c] Chen *et al.*, 1991. [d] Feeney *et al.*, 1990. [e] Fan *et al.*, 1991. [f] Nishiyama *et al.*, 1993. [g] Grimshaw *et al.*, 1992. [h] Clermont *et al.*, 1993. [i] Scrutton *et al.*, 1990. [j] Yaoi *et al.*, 1994. [k] Chen *et al.*, 1995. [l] NA, not applicable since the value cannot be calculated since the authors stated that the wild-type enzyme was inactive with the unnatural form of the coenzyme.

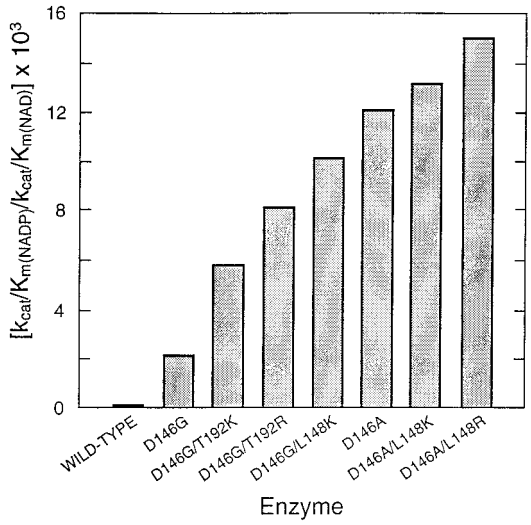

FIGURE 7: Increases in $NADP^+$ specificity that accompanied mutation of residues 146, 148, and 192. $NADP^+$ specificities are expressed as $[k_{cat(NADP)}/K_{m(NADP)}]/[k_{cat(NAD)}/K_{m(NAD)}] \times 10^3$, for wild-type enzyme and the indicated mutant enzymes.

for enzymes D146G, D146S, D146A, and D146N, respectively.

Depending on which nucleotide served as coenzyme, optimal activity of the wild-type enzyme occurred at widely differing pH values. The catalytic efficiency with the unnatural coenzyme ($NADP^+$) was far greater at pH 6 than at pH 9, the optimal pH using NAD^+. Enhanced activity at acidic pH may reflect, in part, decreased charge repulsion between the γ-carboxyl of Asp146 and the 2′-phosphate of $NADP^+$. Consistent with this hypothesis is that when Asp146 was replaced by Ala or Gly, the pH profile using $NADP^+$ reverted to that of wild-type enzyme and of Asp146 mutant enzymes using NAD^+.

Neither mutant enzyme D146N nor D146S exhibited detectable activity with $NADP^+$. The inactivity of enzyme D146N suggests that both the charge and the bulk of Asp146 may discriminate against $NADP^+$. In addition, the 800- and 1500-fold decreases in catalytic efficiency and the increased K_m for NAD^+ are consistent with disruption of the nucleotide-binding site, possibly due to formation of an unfavorable hydrogen bond by the side chain of D146N or D146S.

Inspection of the binary NAD^+:HMG-CoA reductase complex of the wild-type enzyme suggested that the introduction of positive charge at positions 147, 148, 149, or 192 might further enhance the $NADP^+$ specificity of mutant enzymes D146A or D146G. Preliminary molecular modeling, which assumed that substitution of Ala or Gly at position 146 did not perturb backbone ϕ, ψ angles or the direction in which side chains extend, implicated Leu148 and Thr192 as the best candidates for mutation. The side chains of residues 148 and 192 should face the 2′-phosphate of the adenine ribose of $NADP^+$, whereas those of positions 147 and 149 should face away. Enhanced specificity for $NADP^+$ indeed accompanied the introduction of positive charge at position 148 or 192 but not at position 147 or 149. Enhancement resulted not from any further increase in catalytic efficiency with $NADP^+$, but from up to a 2700-fold decrease in catalytic efficiency using NAD^+.

We postulate that the potential enhancement due to introduction of a positive charge at residues 147, 148, 149, or 192 was counterbalanced by damage to critical local structural interactions that disrupt overall dinucleotide binding. In the wild-type enzyme, the solvent-exposed side chain of Gln147 is part of a flexible loop and helix (αF) that appears to clamp on top of the adenine ring when NAD^+ binds. Gln147 makes a hydrogen bond with the backbone carbonyl oxygen of residue 143, potentially stabilizing the loop configuration. Leu148, which is present in αF, appears to provide a hydrophobic contact with the adenine ring of NAD^+ that may contribute to coenzyme binding. On the opposite side of the helix, the side chain of Leu149 extends into the hydrophobic core of the small subunit and so helps to orient helix αF on top of the adenine ring. Thr192 is part of the αG helix that interacts with the pyrophosphate of NAD^+ across the ring of the adenine ribose. Disruption of any or all of these potentially critical interactions might alter dinucleotide binding with resulting decreases in catalytic efficiency.

Figure 7 summarizes the $NADP^+$ specificities of the single mutant enzymes and of the most effective double mutant enzymes of *P. mevalonii* HMG-CoA reductase. The most

effective mutants increased the specificity for $NADP^+$ 3200-, 4500-, 56 000-, 72 000-, and 83 000-fold relative to the wild-type enzyme (Table 1).

The improvement in specificity for $NADP^+$, the unnatural form of the coenzyme for *P. mevalonii* HMG-CoA reductase, was compared to the results of prior attempts to alter the coenzyme specificity of NAD(H)- or NADP(H)-dependent oxidoreductases. Both the improvement in specificity and the ratio of the catalytic efficiency of the mutant enzyme using the unnatural coenzyme to that for the wild-type enzyme using the natural coenzyme were calculated (Table 2). Improvement in specificity for the unnatural coenzyme was expressed as the ratio of $[k_{cat(N)}/K_{m(N)}]/[k_{cat(U)}/K_{m(U)}]$ for each wild-type enzyme to $[k_{cat(N)}/K_{m(N)}]/[k_{cat(U)}/K_{m(U)}]$ for each mutant enzyme, where N and U denote the natural and unnatural forms of the coenzyme, respectively. Catalytic efficiency was expressed as the ratio of $k_{cat(U)}/K_{m(U)}$ for mutant enzymes to $k_{cat(N)}/K_{m(N)}$ for the wild-type enzyme. In all instances, the mutant enzyme selected for comparison was that which showed the greatest improvement in specificity for the unnatural coenzyme. The primary mutation in studies that enhanced NADP(H) utilization by NAD(H)-dependent enzymes was, as in the present study, the change of the aspartate that interacts with the 2′-OH of the adenine ribose of NAD(H) to a residue with an uncharged side chain. Secondary mutations included the introduction of positively charged side chains to stabilize the 2′-phosphate of NADP(H), as was done for *P. mevalonii* HMG-CoA reductase. Conversely, an enhanced ability of NADP(H)-dependent enzymes to utilize NAD(H) followed removal of positively charged residues and the addition of an aspartate in the region surrounding the 2′-OH of the adenine ribose of NAD(H).

For *P. mevalonii* HMG-CoA reductase, our maximum improvement in $NADP^+$ specificity was 83 300-fold for mutant enzyme D146A/L148R. While small relative to the over a million-fold increase for *E. coli* isocitrate dehydrogenase (Chen *et al.*, 1995), this value compares favorably with the enhancement achieved in most other studies for which improvement in specificity could be calculated (Table 2). The efficiency of mutant enzyme D146G using $NADP^+$ was, however, only 0.1% that of the wild-type enzyme using NAD^+, an efficiency lower than that achieved in most other studies, notably the 126% wild-type efficiency of the best mutant of *E. coli* dihydrolipoamide dehydrogenase (Bocanegra *et al.*, 1993). In the above studies, seven and five amino acid changes were made in isocitrate dehydrogenase and dihydrolipoamide dehydrogenase, respectively, suggesting many more mutations in *P. mevalonii* HMG-CoA reductase may be necessary to achieve a comparable change in nucleotide specificity. Further mutations to enhance the catalytic efficiency using $NADP^+$ must, however, await solution of the three-dimensional structures of mutant enzymes D146A and D146G complexed with $NADP^+$, to reveal additional features critical for $NADP^+$ binding and suggest mutations that might further enhance $NADP^+$ specificity.

ACKNOWLEDGMENT

We thank our colleagues Kenneth Bischoff, Dan Bochar, Kenneth Li, Kenneth Rogers, and Scott Rosenthal for helpful suggestions.

REFERENCES

Beach, M., & Rodwell, V. W. (1989) *J. Bacteriol. 171*, 2994−3001.
Bischoff, K. M., & Rodwell, V. W. (1996) *J. Bacteriol. 178*, 19−23.
Bocanegra, J., Scrutton, N., & Perham, R. (1993) *Biochemistry 32*, 2737−2740.
Brown, W. E., & Rodwell, V. W. (1980) in *Dehydrogenases Requiring Nicotinamide Coenzymes* (Jeffery, J., Ed.) pp 232−272, Birkhauser Verlag, Basel.
Cabrera, J. A., Bolds, J., Shields, P. E., Havel, C. M., & Watson, J. A. (1986) *J. Biol. Chem. 261*, 3578−3583.
Chen, R., Greer, A., & Dean, A. (1995) *Proc. Natl. Acad. Sci. U.S.A. 92*, 11666−11670.
Chen, Z., Lee, W., & Chang, S. (1991) *Eur. J. Biochem. 202*, 263−267.
Clermont, S., Corbier, C., Mely, Y., Gerard, D., Wonacott, A., & Branlant, G. (1993) *Biochemistry 32*, 10178−10184.
Devereux, J. P., Haeberli, P., & Smithies, O. (1984) *Nucleic Acids Res. 12*, 387−395.
Fan, F., Lorenzen, J., & Plapp, B. (1991) *Biochemistry 30*, 6397−6401.
Feeney, R., Clarke, A. R., & Holbrook, J. J. (1990) *Biochem. Biophys. Res. Commun. 166*, 667−672.
Gill, J. F., Jr., Beach, M. J., & Rodwell, V. W. (1985) *J. Biol. Chem. 260*, 9393−9398.
Grimshaw, C., Matthews, D., Varughese, K., Skinner, M., Xuong, N., Bray, B., Hoch, J., & Whiteberg, J. (1992) *J. Biol. Chem. 267*, 15334−15339.
Kim, J. P., & Wu, J. (1988) *Proc. Natl. Acad. Sci. U.S.A. 85*, 6677−6681.
Lawrence, C. M., Rodwell, V. W., & Stauffacher, C. V. (1995) *Science 268*, 1758−1762.
Mikaelian, I., & Sergeant, A. (1992) *Nucleic Acids Res. 20*, 376.
Nishiyama, M., Birktoft, J. J., & Teruhiko, B. (1993) *J. Biol. Chem. 268*, 4656−4660.
Rodwell, V. W., Nordstrom, J. L., & Mitschelen, J. J. (1976) *Adv. Lipid Res. 14*, 1−74.
Rossmann, M., Liljas, A., Branden, C.-I., & Banaszak, L. (1975) *Enzymes 11*, 61−102.
Rowland, P., Basak, A. K., Gover, S., Levy, H. R., & Adams, M. J. (1994) *Structure* 2, 1073−1087.
Sambrook, J., Fritsch, E. F., & Maniatis, T. (1989) *Molecular Cloning: A Laboratory Manual*, 2nd ed., Cold Spring Harbor Press, Cold Spring Harbor, NY.
Sanger, F., Nicklen, S., & Coulson, A. R. (1977) *Proc. Natl. Acad. Sci U.S.A. 74*, 5463−5467.
Sayle, R. (1995) RasMol v2.6β, obtained via anonymous ftp from ftp.dcs.ed.ac.uk/pub/rasmol/.
Scrutton, N. S., Berry, A., & Perham, R. N. (1990) *Nature 343*, 38−43.
Wang, Y., Darnay, B. G., & Rodwell, V. W. (1990) *J. Biol. Chem. 265*, 21634−21641.
Yaoi, T., Miyazaki, K., & Oshima, T. (1994) *FEBS Lett. 355*, 171−172.

BI9609937